JACS
JOURNAL OF THE AMERICAN CHEMICAL SOCIETY
Communication
pubs.acs.org/JACS

Reversible, Short α-Peptide Assembly for Controlled Capture and Selective Release of Enantiomers

Xi Chen, Ying He, Yongju Kim,* and Myongsoo Lee*

State Key Lab of Supramolecular Structure and Materials, College of Chemistry, Jilin University, Changchun 130012, China

Supporting Information

ABSTRACT: Although significant progress has been achieved with short peptide nanostructures, the construction of switchable membrane assemblies remains a great challenge. Here we report short α-peptide assemblies that undergo thermo-reversible switching between assembly and disassembly states, triggered by the conformational change of laterally grafted short peptides from a folded α-helix to a random coil conformation. The α-helical peptide based on two oligoether dendron side groups forms flat disks, while the peptide helix based on three dendron side groups forms hollow vesicles. The vesicular membrane can spontaneously capture a racemic mixture through the self-formation of vesicular containers upon heating and enantioselectively release the chiral guest molecule through preferential diffusion across the vesicular walls.

Short peptides that self-assemble into nanostructures are of enormous interest for biological, medical, and biotechnological applications because the design of model peptides exhibiting a high tendency for self-assembled structure formation proved to be an ideal target for mimicking biological activities of proteins.[1] The formation of well-defined peptide assemblies depends critically not only on their amino acid sequence but also on their folded secondary structure. Such assemblies include tubules from cyclic peptides,[2] porous cages from three-armed peptides,[3] nanofibers from sequence-controlled short peptides,[4] vesicles from linear block co-peptides,[5] toroids from cyclic block co-peptides,[6] and nanosheets from collagen mimic short peptides.[7] However, the formation of nanostructures by the self-assembly of such short peptides is mostly based on a β-sheet arrangement of peptide motifs because the folding of short peptides into an α-helical structure is accompanied by a large entropic cost related to the folding of short peptide chains.[8]

Stabilizing the folded forms of short α-peptides is thus prerequisite for the peptide chains to assemble into desired nanostructures.[9] Methods achieved to stabilize α-helical structures include covalent bridging amino acid side chains,[10] metal chelates,[11] helix nucleation,[12] and molecular crowding.[13] In addition to these strategies, cyclization of peptides was also proved to be an efficient approach to stabilizing an α-helical structure through reducing the conformational entropic penalty associated with chain folding.[14] We demonstrated that macrocyclization of the linear peptide precursors with a random coil conformation forces the peptide chains to adopt an α-helical structure.[14] The resulting helical peptides self-assemble into undulated nanofibers through 1-dimensional stacking of elementary micelles. We also showed that cyclization of short peptides through a β-sheet linker induces an α-helical conformation through aggregation of the β-sheet peptides.[6]

However, most of the short α-peptides are far from dynamic conformational switching between random coil and helical states, which is essential for generating switchable peptide nanostructures, because the helical conformation is stabilized by covalent or non-covalent bond stitching that is incompatible with dynamic motion.[10−15] Thus, the challenge in peptide assembly based on α-helical peptides is how to confer dynamic switching functions with their conformations.[16] Considering that the structural transformations of proteins originate from the conformational change of the peptide chains,[17] the design of short α-helical peptides that exhibit high tendencies for medium-induced conformational changes is anticipated to be an ideal target for the construction of dynamic peptide nanostructures. To address this challenge, we considered that lateral grafting of a short α-helical peptide with oligoether dendrons would drive a random coil conformation to fold into an α-helical structure which, in turn, would self-assemble into well-defined peptide nanostructures due to thermal dehydration of oligoether chains.[18] The thermal dehydration of oligoether side chains would force random coil peptide backbones to adopt a helical conformation through enhanced hydrophobic interactions between oligoether side chains and peptide backbones to minimize water influence on α-helical peptide hydrogen bonds.[19] Furthermore, the lateral grafting would drive the induced α-helical peptides to align parallel to the 2-dimensional plane to form anisotropic membrane structures with helical voids between the helical peptide chains.[20]

Here, we report reversible α-peptide nanodisks and vesicles based on flat membrane assembly of α-helical peptides that undergo reversible switching between assembly and disassembly states, triggered by a thermal switch (Figure 1). The self-assembled structures consist of the lateral association of rod-like α-helical peptides which allow the assembly to function as an enantioselective membrane. In particular, the hollow vesicles can spontaneously capture a racemic mixture through the self-formation of membrane walls in response to a thermal signal and enantioselectively release the captured molecule through preferential diffusion across the vesicular walls. The α-helix-forming peptides consist of a KKK$(FAKA)_3$FKKK amino acid sequence with high helix propensity.[21] To endow the peptide chain with a thermo-responsive feature, oligoether dendrons were symmetrically grafted into the peptide chain through click

Received: March 5, 2016
Published: April 14, 2016

DOI: 10.1021/jacs.6b02401
J. Am. Chem. Soc. 2016, 138, 5773−5776

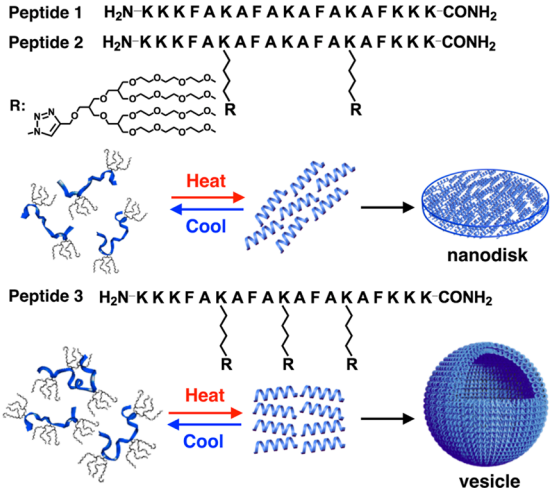

Figure 1. Molecular structures of peptides **1**, **2**, and **3**, with schematic representations of their reversible self-assembly: a nanodisk of peptide **2** and a vesicle of peptide **3**.

chemistry of lysine residues with an oligoether dendron (Figures S1 and S2) . The building blocks were synthesized by a solid-state peptide synthesis method with a combination of both natural amino acids and a dendron-grafted lysine. Peptide **1**, lacking an oligoether dendrimer, adopts a random coil conformation, as confirmed by circular dichroism (CD) measurements, irrespective of temperature change (Figure S3). The α-helical conformation of peptide **1** could be stabilized only in the presence of a stabilizing agent, 2,2,2-trifluoroethanol.

In great contrast, incorporation of oligoether dendrons into the peptide chains drives the random coil conformation of the peptides to switch into an α-helical conformation above a certain temperature (Figure 2). At room temperature, the CD spectrum of peptide **2**, containing two dendrons as side groups, shows a strong minimum at ~196 nm, indicating that the peptide adopts predominantly a random coil conformation. Upon heating to 50 °C, the strong minimum is apparently red-shifted to 208 nm, together with the appearance of another minimum at 222 nm, demonstrating that the random coil conformation of the peptide transforms into an α-helical structure.[22] Similarly, peptide **3**, based on three dendrons as side chains, exhibits a strong negative band at 196 nm at room temperature, demonstrating the peptide is mostly in a random coil conformation. At higher temperatures, the CD spectrum shows two negative bands at 206 and 222 nm, indicating that the peptide is predominantly in an α-helical conformation. It should be noted that the CD intensity at 222 nm of peptide **3** is stronger than that of peptide **2**, suggesting a higher content of α-helical conformation than that of peptide **2**. The results demonstrate that both peptides **2** and **3** undergo conformational switching from random coil to α-helix upon heating. This is attributed to thermal dehydration of the oligoether dendrons. Indeed, the temperature-dependent transmittance of the aqueous solutions of both peptides showed a sharp phase transition at ~45 °C (Figure S4), indicating that the ethylene oxide chains with open conformations are dehydrated to collapse upon heating (Figure S5).

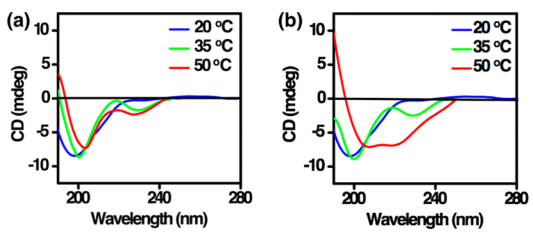

Figure 2. CD spectra of peptides **2** (a) and **3** (b), each in 5 mM aqueous KF solution at various temperatures.

The stabilization of the α-helical conformation upon heating can be understood by considering peptide/water interactions.[19,23,24] The dehydrated oligoether dendrons would interact strongly with the hydrophobic residues such as alanine and phenylalanine of the peptide backbone to reduce the water-accessible surface area. Additionally, the ether oxygens of the dendritic chains would also strongly interact with charged lysine. These interactions provide the shielding effect of the oligoether dendrons on peptide/water interactions to minimize the water influence on peptide hydrogen bonds, which triggers stabilization of α-helices upon heating. This is further supported by the higher CD intensity at 222 nm in peptide **3**, with higher volume fraction of oligoether dendron than that of peptide **2**, indicating that more oligoether dendrons stabilize α-helices more efficiently, consistent with the shielding effect of the oligoether dendrons on peptide/water interactions.

We envisaged that the laterally grafted rod-like α-helical peptides would be aligned parallel to each other to self-assemble into planar nanostructures in which the helical peptides are arranged parallel to the 2D planes.[20,25] To investigate the self-assembled structures of the peptides in aqueous solution including KF, we performed transmission electron microscopy (TEM) experiments. At room temperature, we could not observe any noticeable aggregates, which was additionally confirmed by dynamic light scattering (DLS) measurements, indicating that both peptides exist as molecularly dissolved states at room temperature. Upon heating, the peptides self-assemble into flat membrane structures. The TEM images of peptide **2** showed flat disks with an average diameter of ~80 nm (Figure 3a). Notably, the disk plane has a directionally folded edge, implying that the thermally induced peptide helices are aligned in one direction, parallel to the disk planes (Figure 3d). The formation of the flat nanostructures was also confirmed using cryo-TEM with the vitrified solution, which provides further evidence that the aggregates exist as flat disks in bulk solution (Figures 3b and S6).

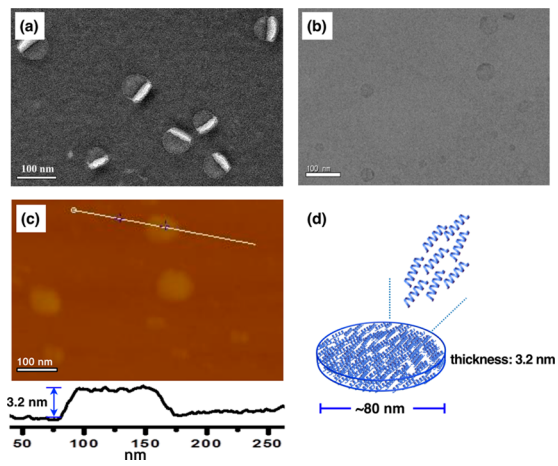

Figure 3. (a) TEM and (b) cryo-TEM image of peptide **2** in 5 mM aqueous KF solution at 50 °C. (c) AFM image and the height profile along the white line (3.2 nm). (d) Schematic representation of the disk assembly of peptide **2**.

DOI: 10.1021/jacs.6b02401
J. Am. Chem. Soc. 2016, 138, 5773−5776

Additional structural information about the disks was obtained by atomic force microscopy (AFM) measurements on hydrophilic mica substrate in the completely dried state (Figure 3c). The AFM image of the peptide revealed flat disks with a thickness of 3.2 nm, which is in reasonable agreement with the expected thickness of roughly single layer packing (Figure 3d). In addition to this example, protein/lipopeptide complexes and metal-coordinated oligopeptides have been reported to form flat nanodisks.[26]

Unlike peptide **2**, which forms flat nanostructures, peptide **3**, based on three dendron side groups, self-assembles into curved vesicular structures, as evidenced by TEM, scanning electron microscopy (SEM), and DLS measurements (Figure 4). When **3** was heated to 50 °C, at which the conformation of the peptide changes into an α-helix, the TEM image stained with uranyl acetate revealed the formation of spherical objects with diameters ranging from 60 to 120 nm. These results indicate that the induced helical conformation triggers the formation of the self-assembled structures. Cryo-TEM investigations confirmed the presence of spherical aggregates with a dark outer circle expected from the 2-D projection of hollow vesicles with a uniform thickness of 3.2 nm. This was further confirmed by X-ray diffraction (XRD) experiments, which showed the *d* value of 3.0 nm (Figure S7). DLS measurements revealed that the aggregates have an average diameter of ~90 nm, which is in reasonable agreement with the size observed by TEM. Considering the calculated molecular dimensions, the peptide helices are arranged parallel to the wall of the vesicle, with hydrophilic oligoether side chains exposed to the water environment. The formation of the nanostructures at higher temperatures was further confirmed using SEM, which provides additional evidence that the aggregates exist as spherical objects (Figure 4c).

To gain insight into the formation of the hollow spherical structure, we performed TEM experiments with a highly diluted condition (0.002 wt%) of peptide **3** (Figure S8). In contrast to peptide **2**, lacking any noticeable aggregates at the identical condition, the image of peptide **3** showed short nanofibers with a uniform diameter of 3.8 nm, demonstrating that the vesicular walls consist of the lateral association of the elementary nanofibers. Considering the calculated length of the peptide helix (3.5 nm), the nanofibers consist of a ribbon-like lateral association of the peptide helices with dendrimer chains located at both faces of the ribbons. With increasing concentration, the elementary nanofibers further assemble through side-by-side interactions to generate a flat membrane structure (Figure 4d).

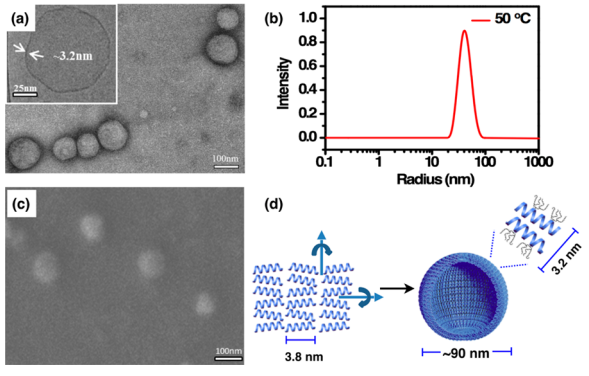

Figure 4. (a) TEM and cryo-TEM (inset) images, (b) DLS, and (c) SEM image of peptide **3** in 5 mM aqueous KF solution at 50 °C. (d) Schematic representation of the vesicular assembly of peptide **3**.

This result implies that the vesicular structure of peptide **3** originates from folding of the flat membranes along two orthogonal directions of the fiber axis and of the helical peptide axis, respectively. Considering that peptide **2**, with less α-helical content, self-assembles into flat disks, the higher α-helical content in peptide **3** plays a key role in the formation of curved vesicles through the lateral association of pre-formed ribbons.

Considering that the vesicular walls consist of parallel arrangements of rod-like α-helical peptides relative to the wall plane, the void spaces formed between the helical peptide arrangements would be chiral.[27] Accordingly, we envisioned that the vesicular walls function as an enantioselective membrane as the one enantiomer over the other one preferentially passes through across the membrane.[27] To corroborate the enantioselective permeability of the vesicular walls, we added racemic 1-(4-bromophenyl)ethanol (5 mM) to a solution of peptide **3** at room temperature (Figure 5). Upon heating of the solution to 55 °C, the peptide molecules self-assemble into hollow vesicles with simultaneous capture of the racemate within their hollow interiors. Encapsulation of the racemate within the vesicular interior was confirmed by high-performance liquid chromatography (HPLC) after separation of the free racemate from the vesicular solution using a Sephadex column (Figure S9). The preferential release of the encapsulated enantiomers was then monitored by tracing HPLC as a function of release time after separation of the vesicles using a Sephadex column. The permeation through the vesicular walls is enantioselective, as shown in Figure 5a, in which the concentrations of both encapsulated enantiomers decrease with increasing permeation time. Notably, the (*R*)-enantiomer diffuses out faster than the (*S*)-enantiomer. After 3 h of separation, the enantioselectivity appears to be at its maximum, and the enantiomeric excess (ee, given in %) reaches 12%. This result demonstrates that the racemic molecule is encapsulated inside the vesicular interior through the spontaneous formation of vesicular walls and then releases out (*R*)-enantiomer selectively. The preferential diffusion of the enantiomer indicates that the vesicular walls

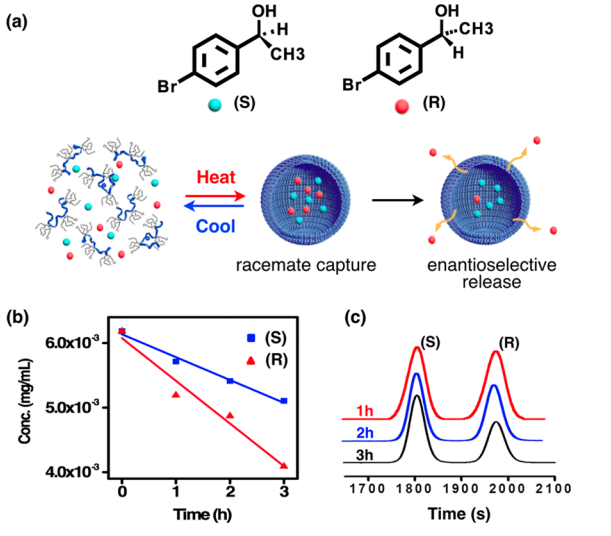

Figure 5. (a) Schematic representation of capture and chiral separation of racemic 1-(4-bromophenyl)ethanol with peptide **3**, and (b) its enantioselective permeation through a chiral membrane assembly of peptide **3**. (c) HPLC chromatograms of racemic 1-(4-bromophenyl)-ethanol at various times.

DOI: 10.1021/jacs.6b02401
J. Am. Chem. Soc. 2016, 138, 5773−5776

allow a chiral environment for the racemate, which is attributed to the lateral arrangements of the short helical peptides.

The results described herein demonstrate that the lateral incorporation of oligoether side groups into a short peptide backbone provides an efficient strategy to allow the short peptides to undergo conformational switching from random coils to α-helices (Figure 1). The switching feature of the peptide conformation is attributed to reversible shielding of the peptide backbone from the water environment by the oligoether dendron side groups. Furthermore, the switchable α-helical peptides self-assemble into reversible membrane structures in which the rod-like α-helices are aligned parallel to each other. Peptide **2**, based on two oligoether dendrons, forms discrete disks, while peptide **3**, based on three dendrons, forms hollow vesicles. The main driving force responsible for the formation of the switchable peptide nanostructures is the reversible stabilization of the α-helical conformation. Importantly, the hollow vesicles formed from peptide **3** can spontaneously capture a racemic mixture through the self-formation of membrane walls upon heating and enantioselectively release the guest molecules through preferential diffusion across the vesicular walls. Considering that most of the membrane nanostructures are far from controlled encapsulation,[27−29] the notable feature of the peptide membranes is their ability to control the capture of racemic molecules through assembly/disassembly switching and enantioselective release the captured molecules. Such a unique peptide assembly will offer opportunities to explore biomedical applications for the controlled capture and release of proteins, genes, and drugs.

■ ASSOCIATED CONTENT

Supporting Information

The Supporting Information is available free of charge on the ACS Publications website at DOI: 10.1021/jacs.6b02401.

Experimental details and characterization data (PDF)

■ AUTHOR INFORMATION

Corresponding Authors

*yjkim@jlu.edu.cn

*mslee@jlu.edu.cn

Notes

The authors declare no competing financial interest.

■ ACKNOWLEDGMENTS

This work was supported by 1000 Program, NSFC (Grant 51473062, Grant 21574055, and Grant 21550110493).

■ REFERENCES

(1) (a) Knowles, T. P. J.; Oppenheim, T. W.; Buell, A. K.; Chirgadze, D. Y.; Welland, M. E. *Nat. Nanotechnol.* **2010**, *5*, 204. (b) Fleming, S.; Ulijn, R. V. *Chem. Soc. Rev.* **2014**, *43*, 8150. (c) Chambron, J.-C.; Meyer, M. *Chem. Soc. Rev.* **2009**, *38*, 1663. (d) Boekhoven, J.; Stupp, S. I. *Adv. Mater.* **2014**, *26*, 1642. (e) Shao, H.; Lockman, J. W.; Parquette, J. R. *J. Am. Chem. Soc.* **2007**, *129*, 1884. (f) Marine, J. E.; Song, S.; Liang, X.; Watson, M. D.; Rudick, J. G. *Chem. Commun.* **2015**, *51*, 14314. (g) Dehsorkhi, A.; Castelletto, V.; Hamley, I. W. *J. Pept. Sci.* **2014**, *20*, 453. (h) Vauthey, S.; Santoso, S.; Gong, H.; Watson, N.; Zhang, S. *Proc. Natl. Acad. Sci. U.S.A.* **2002**, *99*, 5355. (i) Fletcher, J. M.; et al. *Science* **2013**, *340*, 595.

(2) (a) Chapman, R.; Danial, M.; Koh, M. L.; Jolliffe, K. A.; Perrier, S. *Chem. Soc. Rev.* **2012**, *41*, 6023. (b) Hartgerink, J. D.; Granja, J. R.; Milligan, R. A.; Ghadiri, M. R. *J. Am. Chem. Soc.* **1996**, *118*, 43.

(3) Matsuura, K.; Murasato, K.; Kimizuka, N. *J. Am. Chem. Soc.* **2005**, *127*, 10148.

(4) (a) Rufo, C. M.; Moroz, Y. S.; Moroz, O. V.; Stöhr, J.; Smith, T. A.; Hu, X.; De Grado, W. F.; Korendovych, I. V. *Nat. Chem.* **2014**, *6*, 303. (b) Gao, Y.; Zhao, F.; Wang, Q.; Zhang, Y.; Xu, B. *Chem. Soc. Rev.* **2010**, *39*, 3425.

(5) Yoon, Y.-R.; Lim, Y.-B.; Lee, E.; Lee, M. *Chem. Commun.* **2008**, 1892.

(6) Lim, Y.-B.; Moon, K.-S.; Lee, M. *Angew. Chem., Int. Ed.* **2009**, *48*, 1601.

(7) Jiang, T.; et al. *J. Am. Chem. Soc.* **2014**, *136*, 4300.

(8) (a) Abb, S.; Harnau, L.; Gutzler, R.; Rauschenbach, S.; Kern, K. *Nat. Commun.* **2016**, *7*, 10335. (b) Luo, Z.; Zhang, S. *Chem. Soc. Rev.* **2012**, *41*, 4736. (c) Lim, Y.-b.; Lee, M. *J. Mater. Chem.* **2011**, *21*, 11680. (d) Kim, S.; Kim, J. H.; Lee, J. S.; Park, C. B. *Small* **2015**, *11*, 3623. (e) Lim, Y.-B.; Lee, E.; Lee, M. *Angew. Chem., Int. Ed.* **2007**, *46*, 3475. (f) Lim, Y.-b.; Lee, E.; Yoon, Y.-R.; Lee, M. *Angew. Chem., Int. Ed.* **2008**, *47*, 4525.

(9) Mondal, S.; Adler-Abramovich, L.; Lampel, A.; Bram, Y.; Lipstman, S.; Gazit, E. *Nat. Commun.* **2015**, *6*, 8615.

(10) (a) Brown, S. P.; Smith, A. B. *J. Am. Chem. Soc.* **2015**, *137*, 4034. (b) Blanco-Lomas, M.; Samanta, S.; Campos, P. J.; Woolley, G. A.; Sampedro, D. *J. Am. Chem. Soc.* **2012**, *134*, 6960. (c) Spokoyny, A. M.; Zou, Y.; Ling, J. J.; Yu, H.; Lin, Y.-S.; Pentelute, B. L. *J. Am. Chem. Soc.* **2013**, *135*, 5946.

(11) Ousaka, N.; Sato, T.; Kuroda, R. *J. Am. Chem. Soc.* **2008**, *130*, 463.

(12) Fremaux, J.; Mauran, L.; Pulka-Ziach, K.; Kauffmann, B.; Odaert, B.; Guichard, G. *Angew. Chem., Int. Ed.* **2015**, *54*, 9816.

(13) White, S. J.; Johnson, S. D.; Sellick, M. A.; Bronowska, A.; Stockley, P. G.; Wälti, C. *Angew. Chem., Int. Ed.* **2015**, *54*, 974.

(14) Sim, S.; Kim, Y.; Kim, T.; Lim, S.; Lee, M. *J. Am. Chem. Soc.* **2012**, *134*, 20270.

(15) Azzarito, V.; Long, K.; Murphy, N. S.; Wilson, A. J. *Nat. Chem.* **2013**, *5*, 161.

(16) (a) Cerpa, R.; Cohen, F. E.; Kuntz, I. D. *Folding Des.* **1996**, *1*, 91. (b) Kim, W.; Thevenot, J.; Ibarboure, E.; Lecommandoux, S.; Chaikof, E. L. *Angew. Chem., Int. Ed.* **2010**, *49*, 4257.

(17) (a) Gosser, Y.; Hermann, Y.; Majumdar, A.; Hu, W.; Frederick, R.; Jiang, F.; Xu, W.; Patel, D. J. *Nat. Struct. Biol.* **2001**, *8*, 146. (b) Zimenkov, Y.; Dublin, S. N.; Ni, R.; Tu, R. S.; Breedveld, V.; Apkarian, R. P.; Conticello, V. P. *J. Am. Chem. Soc.* **2006**, *128*, 6770.

(18) (a) Kim, Y.; Kang, J.; Shen, B.; Wang, Y.; He, Y.; Lee, M. *Nat. Commun.* **2015**, *6*, 8650. (b) Huang, Z.; Lee, H.; Kang, S.-K.; Nam, J.-M.; Lee, M. *Nat. Commun.* **2011**, *2*, 459.

(19) Hamed, E.; Xu, T.; Keten, S. *Biomacromolecules* **2013**, *14*, 4053.

(20) Lee, E.; Kim, J.-K.; Lee, M. *Angew. Chem., Int. Ed.* **2009**, *48*, 3657.

(21) (a) Marqusee, S.; Robbins, V. H.; Baldwin, R. L. *Proc. Natl. Acad. Sci. U.S.A.* **1989**, *86*, 5286. (b) Pace, C. N.; Scholtz, J. M. *Biophys. J.* **1998**, *75*, 422.

(22) Aili, D.; Enander, K.; Rydberg, J.; Nesterenko, I.; Björefors, F.; Baltzer, L.; Liedberg, B. *J. Am. Chem. Soc.* **2008**, *130*, 5780.

(23) Guzmán, D. L.; Randall, A.; Baldi, P.; Guan, Z. *Proc. Natl. Acad. Sci. U.S.A.* **2010**, *107*, 1989.

(24) Kushner, A. M.; Guan, Z. *Angew. Chem., Int. Ed.* **2011**, *50*, 9026.

(25) Hong, D.-J.; Lee, E.; Jeong, H.; Lee, J.-K.; Zin, W.-C.; Nguyen, T. D.; Glotzer, S. C.; Lee, M. *Angew. Chem., Int. Ed.* **2009**, *48*, 1664.

(26) (a) Castelletto, V.; Hamley, I. W.; Reza, M.; Ruokolainen, J. *Nanoscale* **2015**, *7*, 171. (b) Przybyla, D. E.; Chmielewski, J. *J. Am. Chem. Soc.* **2010**, *132*, 7866.

(27) (a) Shen, J.; Okamoto, Y. *Chem. Rev.* **2016**, *116*, 1094. (b) Li, C.; Cho, J.; Yamada, K.; Hashizume, D.; Araoka, F.; Takezoe, H.; Aida, T.; Ishida, Y. *Nat. Commun.* **2015**, *6*, 8418.

(28) (a) Xie, R.; Chu, L. Y.; Deng, J. *Chem. Soc. Rev.* **2008**, *37*, 1243. (b) Shimomura, K.; Ikai, T.; Kanoh, S.; Yashima, E.; Maeda, K. *Nat. Chem.* **2014**, *6*, 429. (c) Weng, X.; Baez, J. E.; Khiterer, M.; Hoe, M. Y.; Bao, Z.; Shea, K. J. *Angew. Chem., Int. Ed.* **2015**, *54*, 11214.

(29) (a) Nakamura, M.; Kiyohara, S.; Saito, K.; Sugita, K.; Sugo, T. *J. Chromatography A* **1998**, *822*, 53. (b) Higuchi, A.; Higuchi, Y.; Furuta, K.; Yoon, B. O.; Hara, M.; Maniwa, S.; Saitoh, M.; Sanui, K. *J. Membr. Sci.* **2003**, *221*, 207. (c) Sueyoshi, K.; Fukushima, C.; Yoshikawa, M. *J. Membr. Sci.* **2010**, *357*, 90.

DOI: 10.1021/jacs.6b02401
J. Am. Chem. Soc. 2016, 138, 5773−5776